

Figure 5. Isomer possibilities for complexes 13a,b.

It is apparent from these complexes 12, 13, and 14 that N-H addition to iridium(I) will occur with the ligand PNH(CPhO). Although the reaction is apparently induced by intramolecular cyclization, this premise needs to be tested. We have therefore mixed $\text{IrCl}(\text{PPh}_3)_2$ with 1 mol of benzamide or benzanilide, both with and without 1 equiv of added triphenylphosphine. These conditions are designed to mimic those used to prepare complex 12. The first experiment with no added PPh_3 is designed to simulate a pathway for PNH(CPhO) addition where N-H cleavage by $\text{IrCl}(\text{PPh}_3)_2$ is the initial step. The second experimental condition with 1 mol of added PPh_3 reproduces the conditions for a pathway where phosphine complexation is the first step, and N-H addition is induced by $\text{IrCl}(\text{PPh}_3)_3$. The only difference between PNH(CPhO) and these above sets of conditions is the intramolecularity of NH additions from PNH(CPhO). Under the two sets of conditions with added benzamide or benzanilide we observe, by IR spectroscopy, no loss of the amide N-H functionality or the formation of an iridium hydride. Our claim

of intramolecular "chelate-assisted" oxidative addition with PNH(CPhO) therefore appears to be justified.

Now that our finding of iridium(III) hydrides from PNH(CPhO) and iridium(I) complexes is fully justified, we must return to discuss the formation of the hydride complex $\text{IrHCl}(1,5\text{-COD})(\text{PN}(\text{CPhO}))$ (15) from the treatment of $\text{IrCl}(1,5\text{-COD})(\text{PNH}(\text{CPhO}))$ with Dabco. The reaction was carried out with the amido iridium(I) complex $\text{Ir}(1,5\text{-COD})(\text{PN}(\text{CPhO}))$ being the targeted product. Complex 15 shows no IR bands due to $\nu(\text{NH})$ or amide II, but shifted amide I and III bands at 1610 and 1330 cm^{-1} are observed. Medium-intensity bands due to $\nu(\text{IrH})$ are found at 2160 and 2140 cm^{-1} . We do not find a hydride resonance in the ^1H NMR spectrum (CD_2Cl_2 solvent). The phenyl, methylene, and olefinic protons are in the expected regions (Table I). The $^{31}\text{P}\{^1\text{H}\}$ NMR spectrum (CD_2Cl_2 solvent) shows a broad resonance at δ 15.4 ($\nu_{1/2} = 12$ Hz) at 27 $^\circ\text{C}$, which shifts and narrows to δ 9.4 ($\nu_{1/2} = 3$ Hz) at -72 $^\circ\text{C}$. It appears therefore that the complex is undergoing intramolecular exchange, which may explain why the upfield hydride resonance is not observed.¹³

It is not obvious at present as to why this hydride complex, 15, is formed under the identical experimental conditions that can be used to prepare compounds 9, 10, and 11. A plausible explanation is that an initially formed anionic iridium(I) complex $\text{IrCl}(1,5\text{-COD})(\text{PN}(\text{CPhO}))^-$ is protonated at iridium by DabcoH^+ faster than it undergoes chloride ion loss, resulting in the formation of $\text{IrHCl}(1,5\text{-COD})(\text{PN}(\text{CPhO}))$. Nevertheless this explanation remains speculative, and further investigation of these amido complexes of the later transition metals is needed before variations in their reaction chemistry can be fully explained.

Acknowledgment. We thank Dr. F. Mathey (CNRS) for helpful discussions.

(13) Brown, J. M.; Dayrit, F. M.; Lightowler, D. *J. Chem. Soc., Chem. Commun.* 1983, 414-415.

Contribution from the Department of Chemistry and Laboratory for Molecular Structure and Bonding, Texas A&M University, College Station, Texas 77843

Solid-State Structure of $\alpha\text{-Mo}_2\text{Cl}_4(\text{dppe})_2$ and Its Transformation to $\beta\text{-Mo}_2\text{Cl}_4(\text{dppe})_2$. Evidence for the Internal Flip Mechanism

Pradyot A. Agaskar and F. Albert Cotton*

Received May 30, 1985

The crystal structure of $\alpha\text{-Mo}_2\text{Cl}_4(\text{dppe})_2 \cdot \text{OC}_4\text{H}_8$, in which the two dppe ligands chelate each of the Mo atoms of the dimer, has been determined. The space group is $C2/c$ with $a = 32.946$ (5) \AA , $b = 9.876$ (4) \AA , $c = 23.179$ (3) \AA , $\beta = 119.67$ (1) $^\circ$, $V = 6548$ (7) \AA^3 , and $Z = 4$. The midpoint of the Mo-Mo unit resides on an inversion center. The Mo-Mo bond distance is 2.140 (2) \AA , and the mean Mo-P and Mo-Cl distances are 2.548 [2] \AA and 2.423 [1] \AA , respectively. The light brown product of the solid-state transformation of $\alpha\text{-Mo}_2\text{Cl}_4(\text{dppe})_2$ was characterized by its far-IR spectrum, which is identical with that of pure crystalline $\beta\text{-Mo}_2\text{Cl}_4(\text{dppe})_2$. The same transformation in CH_2Cl_2 solution was found to be a reversible process of the first order in both directions. The initial rate constant, assumed to be that of the forward process, was $1.13 \times 10^{-5} \text{ s}^{-1}$, and the rate constant for approach to equilibrium, which is a sum of the rate constants for the forward and reverse processes, was found to be $1.22 \times 10^{-5} \text{ s}^{-1}$. These rates were essentially unaffected by the presence of a 20-fold excess of dppe. These results provide support for our earlier proposal that the isomerization processes occur by an "internal flip" of the Mo_2 unit within the ligand cage.

Introduction

The synthesis of single crystals of both α - and β - $\text{Mo}_2\text{Cl}_4(\text{dppe})_2$, which were originally prepared by Walton and co-workers,¹ and the crystal structure of $\beta\text{-Mo}_2\text{Cl}_4(\text{dppe})_2$ have been described in a previous publication by the present authors.² The isomerization of the α -isomer to the β -isomer in CH_2Cl_2 solution was known to occur³ and has been studied in detail.⁴ A mechanism involving

an internal reorientation (or internal flip) of the Mo_2^{4+} moiety inside the cavity formed by the eight ligand atoms was proposed⁵ for a similar reaction of $\alpha\text{-Mo}_2\text{Br}_4(\text{dppe})_2$ on the basis of the observed first-order nature of the process and other considerations.

(1) Agaskar, P. A.; Cotton, F. A.; Fraser, I. F.; Peacock, R. D. *J. Am. Chem. Soc.* 1984, 106, 1851.

(2) Peacock, R. D., private communication.

(3) Agaskar, P. A.; Cotton, F. A.; Derringer, D. R.; Powell, G. L.; Root, D. R.; Smith, T. J. *Inorg. Chem.* 1985, 24, 2786.

(1) Best, S. A.; Smith, T. J.; Walton, R. A. *Inorg. Chem.* 1978, 17, 99.
(2) Agaskar, P. A.; Cotton, F. A. *Inorg. Chem.* 1984, 23, 3383.

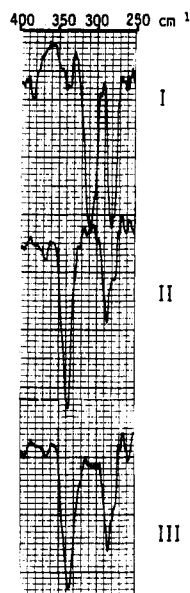


Figure 1. Far-IR spectra of α - $\text{Mo}_2\text{Cl}_4(\text{dppe})_2$ (I), β - $\text{Mo}_2\text{Cl}_4(\text{dppe})_2$ (III), and heat-treated α - $\text{Mo}_2\text{Cl}_4(\text{dppe})_2$ (II).

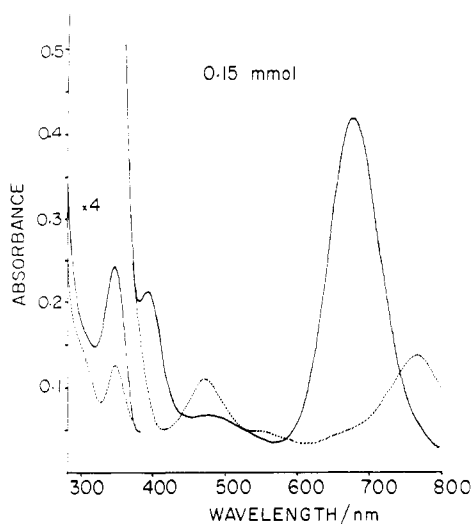


Figure 2. Electronic absorption spectra of α - $\text{Mo}_2\text{Cl}_4(\text{dppe})_2$ (—) and β - $\text{Mo}_2\text{Cl}_4(\text{dppe})_2$ (---).

The isomerization process might be expected to occur also in the solid state if the internal flip mechanism is correct. The isomerization would also be expected to be insensitive to the presence of excess diphosphine ligand. Experiments reported here have confirmed these expectations.

The occurrence of such an internal flip process is of further significance with respect to the racemization of β - $\text{Mo}_2\text{X}_4(\text{PP})_2$ type complexes, some of which are spontaneously resolved on crystallization,⁶ but are apparently subject to rapid racemization when redissolved.

Experimental Procedures

Synthetic methods used to obtain bulk samples, and single crystals of α - $\text{Mo}_2\text{Cl}_4(\text{dppe})_2$ have been described in a previous publication.²

The isomerization of α - $\text{Mo}_2\text{Cl}_4(\text{dppe})_2$ to β - $\text{Mo}_2\text{Cl}_4(\text{dppe})_2$ was effected by heating a sample of the green powder, sealed under vacuum in a Pyrex tube, to 250 °C and maintaining it at that temperature for 2 days. The light brown powder that was obtained was shown to be entirely the β -isomer by its far-IR spectrum, Figure 1.

The same process was observed in CH_2Cl_2 solution by monitoring the UV-visible spectrum of a 0.15 mM solution of α - $\text{Mo}_2\text{Cl}_4(\text{dppe})_2$. The final spectrum observed after a period of 3 days was identical with that of the β -isomer, Figure 2.

Table I. Kinetic Data for the α - to β -Isomerization of $\text{Mo}_2\text{Cl}_4(\text{dppe})_2$ in CH_2Cl_2 Solution

(I) absence of excess dppe		(II) presence of 20-fold excess of dppe	
time/min	absorbance	time/min	absorbance
0	0.425 ^a	0	0.435
280	0.360	290	0.370
460	0.310	470	0.325
1150	0.195	1165	0.215
1470	0.155	1480	0.175
1725	0.135	1730	0.145
1975	0.115	1985	0.125
2675	0.095	2680	0.100
2990	0.085	2995	0.085
4050	0.067	4055	0.060
4465	0.058	4485	0.055

^a $C_{\text{at } t=0} = 1.5 \times 10^{-4}$ mol.

Table II. Summary of Crystallographic Data and Data Collection Procedures

formula	$\text{Mo}_2\text{Cl}_4\text{P}_4\text{C}_{52}\text{H}_{48}\cdot\text{OC}_4\text{H}_8$
fw	1202.66
space group	$C2/c$
syst absences	$hkl, h + k \neq 2n; h0l, l \neq 2n$
<i>a</i> , Å	32.946 (5)
<i>b</i> , Å	9.876 (4)
<i>c</i> , Å	23.179 (3)
α , deg	90.0
β , deg	119.674 (9)
γ , deg	90.0
<i>V</i> , Å ³	6548 (7)
<i>Z</i>	4
<i>d</i> _{calcd} , g/cm ³	1.224
cryst size, mm	$0.3 \times 0.2 \times 0.1$
μ (Mo K α), cm ⁻¹	6.68
data colln instrum	Enraf-Nonius CAD-4
radiation (monochromated in incident beam)	Mo K α
orientation reflns: no.; range (2θ), deg	25; $12 \leq 2\theta \leq 24$
temp, °C	22 ± 3
scan method	$\theta/2\theta$
data colln range (2θ), deg	$4.0 \leq 2\theta \leq 45.0$
no. of unique data, total with $F_o^2 > 3\sigma(F_o^2)$	5533, 1872
no. of params refined	300
transmissn factors: max, min	99.6%, 92.1%
<i>R</i> ^a	0.069
<i>R</i> _w ^b	0.086
quality-of-fit indicator ^c	1.651
largest shift/esd, final cycle	0.3
largest, peak, e/Å ³	0.659

^a $R = \sum ||F_o| - |F_c|| / \sum |F_o|$. ^b $R_w = [\sum w(|F_o| - |F_c|)^2 / \sum w|F_o|^2]^{1/2}$; $w = 1/\sigma^2(|F_o|)$. ^c Quality of fit = $[\sum w(|F_o| - |F_c|)^2 / (N_{\text{observns}} - N_{\text{params}})]^{1/2}$.

Kinetic data for this process were also obtained in the presence of a 20-fold excess of bis(diphenylphosphino)ethane. Both sets of data are listed in Table I.

X-ray Diffraction Procedures

Data Collection. The crystal was placed in a thin-walled glass capillary and surrounded by a mineral oil/THF mixture. It was held in place by a dab of epoxy cement.

Unit cell constants were determined from the geometric parameters of 25 well-centered reflections with 2θ values in the range $10^\circ < 2\theta < 25^\circ$ and are listed in Table II. These were consistent with a *C*-centered monoclinic lattice. The *C*-centering was subsequently confirmed by the systematic absence of *hkl* reflections with $h + k = 2n + 1$. The systematic absences also revealed the presence of a *c*-glide, and the correct space group was determined by a successful refinement to be $C2/c$.

The total number of reflections measured was 5689, of which 156 were intensity standards. Only those unique reflections with a $I/\sigma(I)$ ratio greater than 3, which numbered 1872, were used. Corrections were made for Lorentz and polarization effects. The intensity standards showed a decay of 1.9% over the period of 46.3 h of exposure time, and the data

(6) Cotton, F. A.; Powell, G. L. *Inorg. Chem.* **1983**, *22*, 1507.

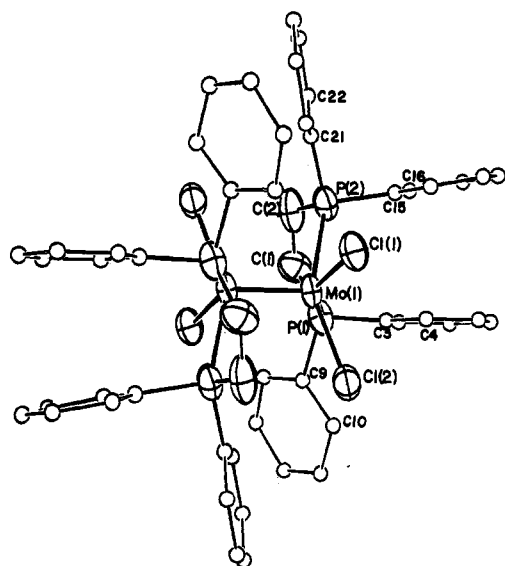


Figure 3. ORTEP drawing of the entire molecule of α - $\text{Mo}_2\text{Cl}_4(\text{dppe})_2$ with thermal ellipsoids at 50% level for Mo, Cl, and P atoms and C(1) and C(2). Those of the atoms in the phenyl rings have been arbitrarily reduced. Unlabeled phenyl carbon atoms follow from those given. Only half the atoms are labeled; the others are related by a center of inversion at the midpoint of the Mo–Mo bond.

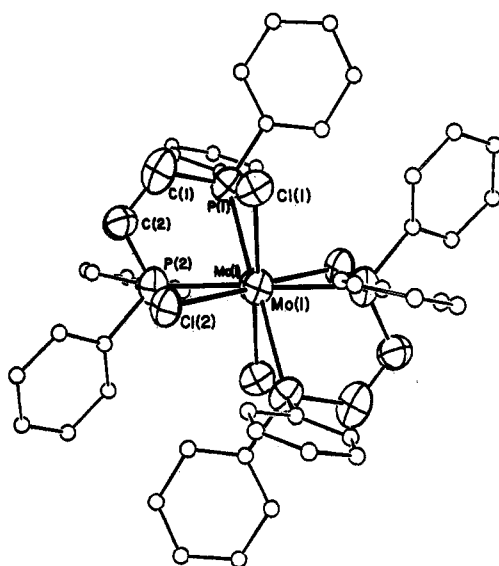


Figure 4. View of the molecule of α - $\text{Mo}_2\text{Cl}_4(\text{dppe})_2$ down the Mo–Mo bond axis.

were corrected to account for this decay. Empirical absorption corrections were applied on the basis of a transmission function derived from azimuthal scans of six reflections with values of the χ -angle around 90° . The maximum and minimum transmission factors were 99.59% and 92.13%, respectively.

Solution and Refinement of the Structure.⁷ The positions of the molybdenum atoms were obtained by using direct methods. The rest of the atoms were located from difference Fourier maps computed after least-squares refinement of atoms already found.

Anisotropic displacement parameters were used for all atoms except those of the THF molecule. The final R factor was 0.069. This is listed in Table II along with all other relevant data. The positional parameters and equivalent isotropic displacement parameters of all atoms are listed in Table III.

Results

The entire molecule is shown in Figure 3, where the atom-numbering scheme is also given. The C_{2h} symmetry of the

Table III. Positional and Thermal Parameters for α - $\text{Mo}_2\text{Cl}_4(\text{dppe})_2 \cdot \text{THF}^a$

atom	x	y	z	B, Å ²
Mo(1)	0.74463 (4)	0.2689 (2)	0.45124 (5)	3.79 (3)
Cl(1)	0.8173 (1)	0.3333 (5)	0.4573 (2)	4.9 (1)
Cl(2)	0.7154 (1)	0.4977 (5)	0.4154 (2)	5.1 (1)
P(1)	0.6615 (1)	0.1825 (5)	0.3799 (2)	4.7 (1)
P(2)	0.7533 (1)	0.0288 (5)	0.4178 (2)	4.5 (1)
O(1)	0.576 (1)	0.246 (4)	0.783 (2)	35 (2)*
C(1)	0.6577 (5)	-0.001 (2)	0.3906 (8)	5.9 (5)
C(2)	0.7055 (5)	-0.078 (2)	0.4161 (6)	6.2 (5)
C(3)	0.6449 (5)	0.204 (2)	0.2937 (6)	5.7 (5)
C(4)	0.6708 (6)	0.279 (2)	0.2734 (7)	6.1 (5)
C(5)	0.6586 (6)	0.290 (2)	0.2060 (7)	7.4 (6)
C(6)	0.6177 (6)	0.225 (2)	0.1564 (8)	8.9 (7)
C(7)	0.5897 (6)	0.149 (3)	0.1774 (8)	8.9 (7)
C(8)	0.6035 (5)	0.134 (2)	0.2443 (8)	7.3 (6)
C(9)	0.6074 (4)	0.251 (2)	0.3735 (6)	6.6 (5)
C(10)	0.5912 (6)	0.375 (2)	0.3391 (9)	8.4 (7)
C(11)	0.5462 (7)	0.424 (3)	0.3297 (9)	11.0 (8)
C(12)	0.5189 (7)	0.339 (3)	0.350 (1)	10.8 (9)
C(13)	0.5361 (6)	0.213 (3)	0.382 (1)	10.6 (8)
C(14)	0.5816 (5)	0.167 (2)	0.3960 (8)	7.9 (6)
C(15)	0.7448 (5)	0.026 (2)	0.3331 (6)	4.8 (4)
C(16)	0.7085 (5)	-0.053 (2)	0.2830 (6)	6.1 (5)
C(17)	0.7044 (6)	0.054 (2)	0.7177 (7)	6.5 (6)
C(18)	0.7348 (5)	0.020 (2)	0.2061 (7)	6.7 (6)
C(19)	0.7701 (6)	0.090 (2)	0.2561 (7)	7.7 (6)
C(20)	0.7755 (5)	0.098 (2)	0.3213 (6)	5.6 (5)
C(21)	0.8048 (5)	-0.074 (2)	0.4563 (6)	4.5 (4)
C(22)	0.8006 (6)	-0.212 (2)	0.4447 (7)	6.0 (5)
C(23)	0.8423 (6)	-0.297 (2)	0.4734 (7)	7.0 (5)
C(24)	0.8862 (6)	-0.244 (2)	0.5119 (8)	7.6 (6)
C(25)	0.8895 (7)	-0.107 (3)	0.5241 (9)	10.0 (8)
C(26)	0.8477 (5)	-0.012 (2)	0.4951 (8)	7.2 (6)
C(27)	0.545 (1)	0.227 (4)	0.687 (2)	20 (1)*
C(28)	0.569 (2)	0.261 (6)	0.551 (3)	31 (3)*
C(29)	0.590 (1)	0.343 (5)	0.697 (2)	24 (2)*
C(30)	0.609 (1)	0.341 (5)	0.775 (2)	21 (1)*

^aStarred values denote isotropically refined atoms. The isotropic equivalent displacement parameters of the anisotropically refined atoms correspond to the expression $B = \frac{4}{3}[a^2B(1,1) + b^2B(2,2) + c^2B(3,3) + ab(\cos \gamma)B(1,2) + ac(\cos \beta)B(1,3) + bc(\cos \alpha)B(2,3)]$.

Table IV. Principal Bond Distances (Å) and Bond Angles (deg)

Bond Distances			
Mo(1)–Mo(1)'	2.140 (2)	Mo(1)–P(1)	2.544 (4)
–Cl(10)	2.411 (5)	–P(2)	2.553 (5)
–Cl(2)	2.436 (5)		
Bond Angles			
Mo(1)–Mo(1)–Cl(1)	110.1 (1)	Cl(1)–Mo(1)–P(1)	147.5 (2)
–Cl(2)	110.6 (1)	–P(2)	90.4 (2)
–P(1)	101.0 (1)	–Cl(2)	89.3 (2)
–P(2)	100.0 (1)	Cl(2)–Mo(1)–P(1)	88.4 (1)
P(1)–Mo(1)–P(2)	74.8 (2)	–P(2)	147.4 (1)

molecule is clearly seen. Figure 4 shows a view of the molecule down the Mo–Mo bond. It can be seen here that though the Mo–L bonds of the halves of the dimer are not eclipsed, the average L–Mo–Mo–L torsion angle is zero.

Table IV is a list of important bond distances and bond angles. The Mo–Mo bond distance of 2.140 (2) Å is almost exactly the same as that in $\text{Mo}_2\text{Cl}_4(\text{dppm})_2$, 2.138 (1) Å, which also has an eclipsed $\text{Mo}_2\text{Cl}_4\text{P}_4$ core.⁸ The average Mo–Cl bond distance, 2.423 [1] Å, is longer than the corresponding distance in the β -isomer,² while the average Mo–P distance, 2.548 [2] Å, is shorter. Such differences are also seen in the tungsten analogues,⁹ and imply that the phosphine ligand exerts a greater structural trans effect than the chlorine ligand.

The eight ligand atoms form an almost perfect cube, and an alternative set of positions for the Mo atoms can be calculated

(7) All computations were carried out by using programs of the VAX-SDP package on a VAX 11/780 computer. The direct-methods program MULTAN-82 was used.

(8) Abbott, E. H.; Bose, K. S.; Cotton, F. A.; Hall, W. T.; Sekutowski, J. C. *Inorg. Chem.* **1978**, *17*, 3240.

(9) Cotton, F. A.; Felthouse, T. R. *Inorg. Chem.* **1981**, *20*, 3880.

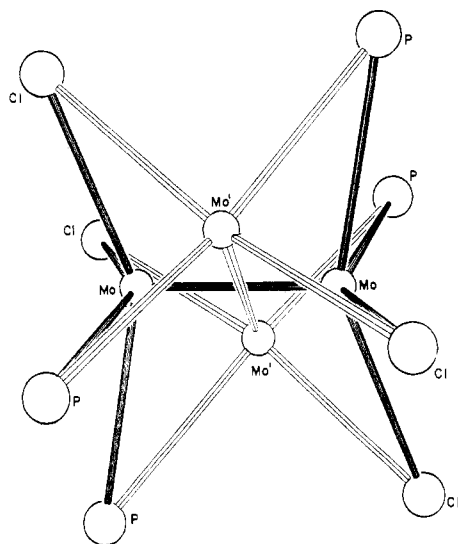


Figure 5. Central core of the molecules with calculated alternative positions for Mo atoms drawn in. The Mo atoms and the shaded bonds show a core with the actual α -structure, while the Mo' atoms and unshaded bonds show a β -structure obtained merely by flipping the Mo_2 unit 90° .

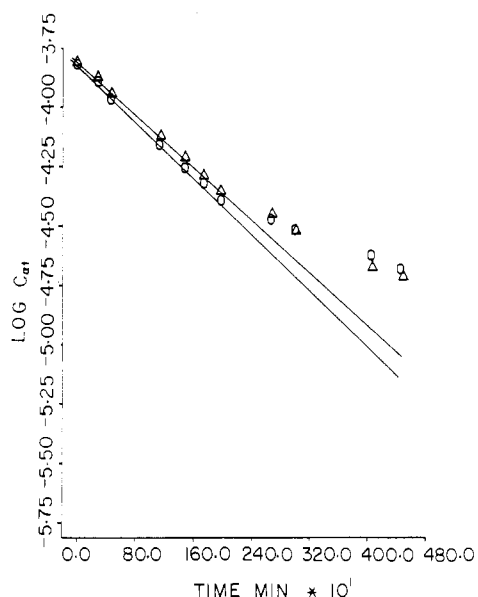


Figure 6. Plot of $\log C_{at}$ vs. time (min): (O) data without excess dppe; (Δ) data in the presence of a 20-fold excess of dppe.

such that the Mo-L bonds are all around 2.5 \AA and the Mo-Mo bond distance is about 2.18 \AA . This is illustrated in Figure 5. The molecule formed when the Mo atoms are put in these calculated positions is of the bridged β -type.

The isomerization process was followed as a function of time at $23 \pm 1^\circ \text{C}$ by measuring the absorbance at the maximum of the $\delta \rightarrow \delta^*$ transition for the α -isomer (677.6 nm). Figure 6 is a plot of $\log C_{at}$ vs. time, where C_{at} is the concentration of the α -isomer at time t . The circles are the data points in the absence of excess dppe, and the triangles are the data points in the presence of a 20-fold excess of dppe. It is apparent that in neither case do the points fit a straight line. However, the first three points in both cases do so with correlation coefficients of >0.99 . The slopes, which are assumed to be the rate of the forward process, are $1.13 \times 10^{-5} \text{ s}^{-1}$ (circles) and $1.03 \times 10^{-3} \text{ s}^{-1}$ (triangles). Figure 7 shows a plot of $\log (C_{at} - C_{aeq})$ vs. time, where C_{at} is the same as described above and C_{aeq} is the concentration of the α -isomer at equilibrium. In this plot, if C_{aeq} is taken to be $0.1 C_{at=0}$, all 11 points, in both cases, can be fitted to a straight line. The correlation coefficients are 0.996 and 0.999, respectively. The slopes of the two linear regression lines are both $1.22 \times 10^{-5} \text{ s}^{-1}$.

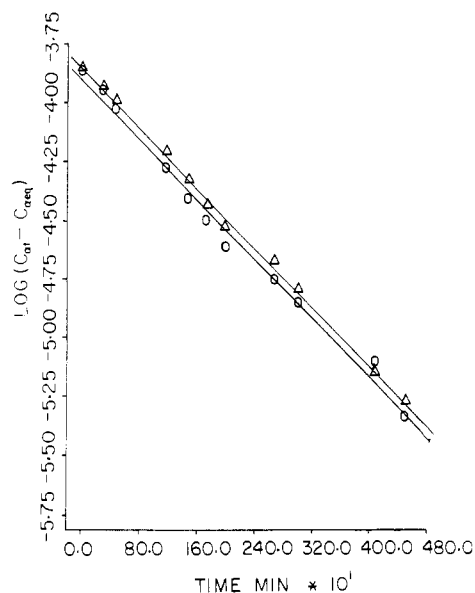


Figure 7. Plot of $\log (C_{at} - C_{aeq})$ vs. time (min).

The slopes in this plot are the sum of the rate constants in the forward and reverse direction, and hence the rates of the reverse processes are $0.9 \times 10^{-6} \text{ s}^{-1}$ (circles) and $1.9 \times 10^{-6} \text{ s}^{-1}$ (triangles), respectively. The equilibrium constants calculated from these rates are 12.5 and 5.4, reasonably close to the value used to generate these plots, given that the initial rate constants were calculated on the basis of only three points.

Discussion

Although our earlier work² with the $\text{Mo}_2\text{Cl}_4(\text{dppe})_2$ system allowed us to obtain crystalline samples of both the α and the β isomers, our interest at that time was entirely concentrated on the β isomer because of its ring conformational properties and their relationship to the optical activity of such molecules.³ Subsequently, however, when the fact that $\alpha\text{-M}_2\text{X}_4(\text{dppe})_2$ isomers isomerize unimolecularly to the $\beta\text{-M}_2\text{X}_4(\text{dppe})_2$ isomers was recognized,^{4,5} and we were led to suggest⁵ as a mechanism a simple internal flip of the M_2 unit within the ligand cage, our interest in $\alpha\text{-Mo}_2\text{Cl}_4(\text{dppe})_2$ was stimulated. In particular, we felt that studies of the $\alpha \rightarrow \beta$ isomerization for this system could provide further tests of our proposed flip mechanism.

As a basis for the study of the isomerization we first established the crystal and molecular structure of $\alpha\text{-Mo}_2\text{Cl}_4(\text{dppe})_2$. The α and β isomers of this compound constitute only the second such pair to be structurally characterized. The first ones were the homologous isomeric $\text{W}_2\text{Cl}_4(\text{dppe})_2$ compounds.⁹ While $\beta\text{-Mo}_2\text{Cl}_4(\text{dppe})_2$ and $\beta\text{-W}_2\text{Cl}_4(\text{dppe})_2$ are isomorphous,^{2,9} that is not true for the α -isomers, since different molecules of solvation are present in each case. For $\alpha\text{-W}_2\text{Cl}_4(\text{dppe})_2$ there were four molecules of the complex and two molecules of water in each unit cell, while in the crystalline material studied here there are four molecules of the complex and four molecules of tetrahydrofuran in the unit cell.

The $\alpha\text{-Mo}_2\text{Cl}_4(\text{dppe})_2$ and $\alpha\text{-W}_2\text{Cl}_4(\text{dppe})_2$ molecules themselves, however, are isostructural. In each case the molecules are crystallographically centrosymmetric, and they differ only in the exact values of bond lengths and angles involving the metal atoms. The W-W distance is $0.140 (2) \text{ \AA}$ longer than the Mo-Mo distance, which is about as expected,^{10,11} although in most other cases the difference is only about 0.10 \AA and often less. On the other hand the W-Cl and W-P distances are slightly shorter than the corresponding Mo-Cl and Mo-P distances, which is a well-established¹¹ if slightly surprising relationship in compounds of this class.

(10) Cotton, F. A.; Walton, R. A. "Multiple Bonds Between Metal Atoms"; Wiley: New York, 1982.

(11) Cotton, F. A.; Extine, M. W.; Felthouse, T. R.; Kolthammer, B. W. S.; Lay, D. G. *J. Am. Chem. Soc.* **1981**, *103*, 4040.

The most likely alternative to our previously suggested internal flip mechanism for the $\alpha \rightarrow \beta$ interconversion would be a process in which one or both of the ligands would break at least one of their M–P bonds. It seems to us that for any process of the latter type, two predictions could be made. (1) It would not proceed cleanly in the solid state. (2) If such a process occurred in solution, it is likely that the presence of a large excess of dppe would affect the rate of isomerization, probably in the sense of retarding it. On the other hand, for the internal flip mechanism, isomerization would be possible in the solid state, and in solution the presence of excess dppe should have no influence on the rate. Experimental tests have been carried out relating to both of these points.

When green α - $\text{Mo}_2\text{Cl}_4(\text{dppe})_2$ was heated under static vacuum at 250 °C it was converted completely and without decomposition to brown β - $\text{Mo}_2\text{Cl}_4(\text{dppe})_2$, as monitored by the color change and by the infrared spectrum (Figure 1) of the product after 2 days of heating. If dissociation and recombination of dppe ligands were required for isomerization to occur, it seems extremely unlikely that such a clean, quantitative conversion would occur. The fact that isomerization occurs by a flip mechanism in the solid does not, of course, require that this be the only mechanism for isomerization in solution.

In CH_2Cl_2 solution, as shown in Figures 6 and 7, the first-order conversion of the α - to the β -isomer and the approach to equilibrium are quantitatively the same in the presence of a 20-fold molar excess of dppe and in the absence of any added dppe. Clearly, any mechanism entailing the initial dissociation of an entire dppe molecule is ruled out. In addition, it would seem unlikely that even a process in which only one end of one dppe or only one Cl^- ligand would have to come adrift to initiate the process could fail to be retarded by the presence of so much dppe in the environment, since the vacancy created by this initial dissociation would be promptly filled by a dppe molecule to give either $\text{Mo}_2\text{Cl}_4(\text{dppe})_3$ or $\text{Mo}_2\text{Cl}_3(\text{dppe})_3$, which would be unable to contribute to the isomerization process.

Acknowledgment. We are grateful to the National Science Foundation for financial support.

Registry No. α - $\text{Mo}_2\text{Cl}_4(\text{dppe})_2 \cdot \text{OC}_4\text{H}_8$, 99531-95-0; α - $\text{Mo}_2\text{Cl}_4(\text{dppe})_2$, 64490-77-3.

Supplementary Material Available: Tables of displacement parameters, structure factors, and complete bond lengths and angles (14 pages). Ordering information is given on any current masthead page.

Contribution from the Department of Chemistry, University of Nottingham, Nottingham NG7 2RD, England, and Inorganic Chemistry Laboratory, University of Oxford, Oxford OX1 3QR, England

Peroxo and Dioxo Metal Carbonyl Intermediates in the Photooxidation of Matrix-Isolated $\text{M}(\text{CO})_6$ ($\text{M} = \text{Cr}, \text{Mo}, \text{W}$) in the Presence of Dioxygen: A Vibrational Spectroscopic Study Using ^{18}O

Matthew J. Almond,^{1a} Joseph A. Crayston,^{1b,c} Anthony J. Downs,^{*1a} Martyn Poliakoff,^{*1b} and James J. Turner^{*1b}

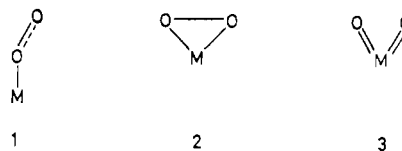
Received June 5, 1985

The photolysis of $\text{M}(\text{CO})_6$ molecules ($\text{M} = \text{Cr}, \text{Mo}, \text{W}$) isolated in O_2 -doped Ar or CH_4 matrices at 10–20 K has been monitored by reference to the IR, Raman, and UV-visible spectra of the matrices. These spectra indicate that the oxidation of $\text{M}(\text{CO})_6$ to binary oxide molecules like MO_2 ($\text{M} = \text{Cr}, \text{Mo}$) and MO_3 ($\text{M} = \text{Mo}, \text{W}$) proceeds via four oxo-carbonyl intermediates, A–D. B has already been shown to be a *trans*-dioxo metal tetracarbonyl, $\text{M}(\text{O})_2(\text{CO})_4$ ($\text{M} = \text{Mo}, \text{W}$). Isotopic enrichment with ^{18}O indicates that (i) A is a peroxo-metal species, $(\eta^2\text{-O}_2)\text{M}(\text{CO})_x$, where x is probably 4 and the molecular symmetry C_{2v} , (ii) C is a dioxo metal carbonyl, $\text{M}(\text{O})_2(\text{CO})_y$, where y is probably 3, and (iii) D is a dioxo metal dicarbonyl, $\text{M}(\text{O})_2(\text{CO})_2$ (the Cr version of which has been characterized previously). Hence we propose a unified reaction scheme for the matrix photooxidation of all three metal hexacarbonyls. Differences in behavior stem in part from differences in the photolability of the intermediates, but the intermediate $\text{Cr}(\text{O})_2(\text{CO})_2$, D, is favored under conditions where Mo and W favor the 18e species *trans*- $\text{M}(\text{O})_2(\text{CO})_4$, B.

Introduction

There is intense interest in finding transition-metal catalysts for the selective oxidation of organic substrates.² One of the few successful autoxidation processes is the epoxidation of ethylene catalyzed by Ag. For a selective catalyst, it is desirable that both dioxygen and the substrate should bind reversibly to the transition-metal center so that oxidation of the substrate can take place. In order to probe the types of *unstable* dioxygen complexes that may be active catalytic intermediates, coordinatively unsaturated metal complexes have been allowed to react with dioxygen and the products immobilized in low-temperature matrices. For example, matrix cocondensation of metal atoms³ with O_2 gives rise to molecules that may emulate some of the different types of active centers created by adsorption of O_2 on a metal surface. Matrix experiments have also revealed a wide range of metal– O_2 interactions in the adducts that O_2 forms with metalloporphyrins.⁴

Such matrix products derived from thermal reactions of O_2 are typically metal–dioxygen complexes involving either η^1 coordination (superoxo, 1) or η^2 coordination (peroxo, 2) of the O_2 ligand.



A different picture emerges from sputtering experiments involving matrix trapping of the species generated when a stream of dioxygen enters the discharge region of a hollow metal cathode: the IR spectra of these species suggest that they are not metal–dioxygen compounds but that the O–O bond has been ruptured to form binary metal oxide molecules, e.g., 3.⁵

Unfortunately, partial aggregation of the unsaturated metal centers is an unavoidable complication in many of these cocondensation experiments. Hence we have favored a different technique for generating the metal centers that overcomes this problem. Our technique involves UV photolysis of a metal car-

(1) (a) University of Oxford. (b) University of Nottingham. (c) Present address: Department of Chemistry, Massachusetts Institute of Technology, Cambridge, MA 02139.

(2) Sheldon, R. A.; Kochi, J. K. *Metal-Catalyzed Oxidations of Organic Compounds*; Academic Press: New York, 1981.

(3) (a) Huber, H.; Klotzbücher, W.; Ozin, G. A.; Vander Voet, A. *Can. J. Chem.* **1973**, *51*, 2722. (b) Tevault, D. E.; Smardzewski, R. R.; Urban, M. W.; Nakamoto, K. *J. Chem. Phys.* **1982**, *77*, 577.

(4) Watanabe, T.; Ama, T.; Nakamoto, K. *J. Phys. Chem.* **1984**, *88*, 440.
(5) Green, D. W.; Ervin, K. M. *J. Mol. Spectrosc.* **1981**, *89*, 145.